Applied Biochemistry and Biotechnology (2019) 187:1193–1203
https://doi.org/10.1007/s12010-018-2871-7

Nanofibrous Scaffolds with Biomimetic Composition for Skin Regeneration

Shahla Khalili[1,2] · Saied Nouri Khorasani[1] · Seyed Mohammad Razavi[3] · Batool Hashemibeni[4] · Ali Tamayol[2]

Received: 28 June 2018 / Accepted: 20 August 2018 /
Published online: 5 September 2018

Abstract

Treatments of skin injuries caused by trauma and diseases are among the most considerable medical problems. The use of scaffolds that can cover the wound area and support cellular ingrowth has shown great promise. However, mimicking the physicochemical properties of the native skin extracellular matrix (ECM) is essential for the successful integration of these scaffolds. Elastin has been known as the second main protein-based component of the native skin ECM. In this research, scaffolds containing gelatin, cellulose acetate, and elastin were fabricated using electrospinning. Subsequently, the effects of soluble elastin on the physical, mechanical, and biological properties of the prepared scaffolds were studied. The results confirmed that the presence of elastin in the composition changed the fiber morphology from straight to ribbon-like structure and decreased the swelling ratio and degradation rate of the scaffold. In vitro experiments showed that elastin-containing scaffolds supported the attachment and proliferation of fibroblast cells. Overall, the obtained results suggest the ternary blend of gelatin, cellulose acetate, and elastin as a good candidate for skin tissue engineering.

Keywords Skin tissue engineering · Elastin · Gelatin · Cellulose acetate · Scaffolds

✉ Saied Nouri Khorasani
saied@cc.iut.ac.ir

Shahla Khalili
shahla.khalili@ce.iut.ac

Seyed Mohammad Razavi
razavi@dnt.mui.ac.ir

Batool Hashemibeni
Hashemibeni@med.mui.ac.ir

Ali Tamayol
atamayol@mit.edu

Back Affiliation

Introduction

Skin is the largest organ in mammalians with a role of protecting the internal organs from environmental pathogens and toxins. Skin injuries due to burn, trauma, and large and deep cuts disturb the skin function and expose the patients to life-threatening conditions. Although skin possesses excellent regenerative properties, underlying conditions such as diabetes and the noticeable size of the damage can prevent the timely healing process. To assist the fast healing of such wounds, dermal scaffolds have been engineered to provide an efficient cover of the wounds and protect the body temporarily yet supporting cellular ingrowth and tissue regeneration [1, 2]. To achieve this goal, numerous efforts have been carried out to create dermal and epidermal substitutes to mimic human skin. Various natural and synthetic materials have been used as substitutes [3, 4]. However, it is known that the composition and architecture of the employed scaffolds affect their success in inducing tissue regeneration. The native ECM is a three-dimensional (3D) protein-rich nanofibrous structure such as collagen and elastin as well as polysaccharides [5].

Elastin is one of the main constituents of skin ECM structural proteins which contributes due to its high elasticity. Elastin, in native tissues, is highly cross-linked and insoluble. In addition, elastin-based constructs offer elastic mechanical properties and excellent biological activity that make them suitable for tissue engineering applications [6, 7]. Furthermore, gelatin, a natural biocompatible protein derived from denaturing of triple helix structure of collagen, is one of the most widely used proteins in tissue engineering applications. Gelatin is cost-effective yet offers biological activity comparable to collagen and can be easily employed in various fabrication processes such as electrospinning [8–12].

Cellulose and its derivatives including cellulose acetate (CA) are the most abundant renewable polysaccharides which have been utilized for the decades in various applications especially as wound dressing materials [13, 14]. Blends of proteins such as gelatin and cellulose acetate have been previously employed for various tissue engineering applications. Our previous study showed that the gelatin/CA blend containing 30%wt CA suggested a good candidate for fabrication of nanofibrous scaffolds for skin tissue engineering [5, 15]. The nanofibrous mats formed by electrospinning process offer architectures similar to native ECM [16]. We hypothesized that the addition of elastin to the blend of gelatin/CA can further improve the elasticity and biological behavior of the scaffold.

To evaluate this hypothesis, we fabricated the nanofibrous scaffolds containing gelatin/CA/elastin using electrospinning. We then studied the effect of elastin incorporation on the physical and biological properties of the ternary blend scaffold. Morphology, swelling, and degradation ratio and tensile properties of the scaffolds were also analyzed. After that, cell viability and growth on the scaffolds were studied using the MTT assay. The attachment and growth of fibroblast cells on the scaffolds were also assessed using SEM micrographs. The results confirmed that the developed mats can be used for engineering biological skin and treatment of skin injuries and disorders.

Experimental Section

Materials

Gelatin type A from porcine skin (Fluka), cellulose acetate (Mr = 29,000; acetyl groups of 39.8%), and soluble α-elastin from bovine neck ligament (Sigma-Aldrich) was used in fabrication of the

scaffolds. Glacial acetic acid (Merck) and glutaraldehyde (GA, 25% *v/v*) (Sigma-Aldrich) were used as solvent and cross-linking agent, respectively, through the fabrication process.

Scaffold Fabrication

CA, gelatin, and elastin were firstly dissolved in 89% (*v/v*) acetic acid at total concentration of 20% (wt/v). The weight ratio of CA to gelatin was constantly kept at 30%, while the ratio of elastin to gelatin was changed from 0 to 10% (wt/wt). Formulation of the samples and their assigned codes are listed in Table 1.

Electrospinning (Fanavaran Nanomeghyas Co., Iran) method was used to fabricate the nanofibrous scaffolds at the applied high voltage of 19.5 kV and a gap distance of 15.5 cm according to the optimization which was achieved in our previous study [5]. The polymer solution was loaded into a 1-mL syringe attached to a 23G blunted stainless steel needle at a flow rate of 1.0 mL/h. The fibers were collected on an aluminum film. Scaffolds were exposed to glutaraldehyde (GA) vapor (25% v) at 40 °C for 6 h for cross-linking and then washed with 0.2 M glycine and phosphate-buffered saline (PBS) to eliminate any unreacted GA.

Scaffold Characterization

The microstructure of the fabricated scaffolds was evaluated using scanning electron microscopy (SEM, Philips XL30) at an accelerating voltage of 20 kV after gold coating (Sputter Coater, BAL-TEC SCD005). The fiber diameters and the pore size of the scaffolds before and after cross-linking were determined by the SEM images using image analysis program (ImageJ, National Institutes of Health, USA) using at least 100 measurements. The pore size of the scaffolds was determined by measuring the diameter of a virtual sphere between fibers in the same or the nearby plane. The distributions and the mean values were determined using IBM SPSS statistics software (version 22).

ATR-Fourier transform infrared spectroscopy tests (ATR-FTIR, Bruker USA) were performed to identify the functional groups of the polymers and prove the cross-linking reaction in the scaffolds over the range of 4000–600 cm^{-1}.

In vitro swelling and degradation of the cross-linked scaffolds were also evaluated from the mass change of samples ($n = 5$) for 21 days according to ASTM F1635. The samples were immersed in PBS (pH 7.4) at 37 °C in an incubator. The solution was refreshed every 3 days. After the specified time intervals, the samples were removed and weighted (W_s) and dried in a vacuum oven and then weighted again (W_d).

The swelling and degradation percents were calculated from Eqs. 1 and 2, respectively:

$$\text{Swelling ratio } (\%) = [W_s - W_i]/W_i \times 100 \quad (1)$$

$$\text{Degradation ratio } (\%) = [W_i - W_d]/W_i \times 100 \quad (2)$$

where W_i is the initial dry weight of the sample before immersion in PBS.

Table 1 Formulation of the samples

Samples	0%	5%	10%
CA/gelatin (%wt/wt)	30%	30%	30%
Elastin/gelatin (%wt/wt)	0%	5%	10%

The mechanical properties of the cross-linked scaffolds were characterized using a tensometer (Zwick 1446-60), with a load cell of 20 N at 10 mm/min strain rate according to ASTM D638. The scaffolds were cut in rectangular shapes (10 × 50 mm) and their thickness was measured at three random points of each sample. At least five samples were prepared for each composition. The tensile properties were measured at wet condition. The samples were soaked in PBS at 37 °C for 2 days prior to the test. The tensile modulus was calculated from the slope of the linear section of the stress-strain curves while the ultimate tensile strength and elongation at break were also measured and reported.

Cell Viability, Attachment, and Proliferation

Scaffolds were cut in a circular shape with a diameter of 15 mm and placed in a 24-well plate and subsequently sterilized for 2 h in 70% (*v*/*v*) ethanol followed by overnight under UV light. The scaffolds were then immersed in culture medium consisting of RPMI (Gibco) supplemented with 10% (*v*/*v*) fetal bovine serum (FBS, Gibco) and 1% (*v*/*v*) penicillin-streptomycin (Invitrogen) overnight prior to cell seeding [4].

The human gingival fibroblasts (HGF) were cultured in RPMI culture medium, at 37 °C, with atmosphere of 5% CO_2 and 90% relative humidity. They were then collected from the flask using Trypsin-EDTA (Sigma), and counted and seeded on the samples ($n = 5$) with a density of 1×10^4 cells per well.

Cellular viability and cytocompatibility of scaffolds were evaluated using MTT assay. The samples were incubated for 1, 3, and 7 days at 37 °C and the atmosphere of 5% CO_2. At each time interval, 40 μL of MTT solution (5 mg/mLit) was added to the samples and incubated for 4 h. After that, 400 mL DMSO was added to dissolve the Formazan product. The absorbance of the product was measured at 570 nm using a spectrophotometer (Hiperion MPR4). Tissue culture plate and DMSO were used to determine the background noise.

Cellular adhesion to the scaffolds and their morphology were observed using SEM micrographs after 1 and 7 days of cell seeding. Samples were fixed with 2.5% (*v*/*v*) glutaraldehyde for 1 h and then dehydrated with graded ethanol (70, 80, 90, and 99.8% *v*/*v*). The samples were then dried in a vacuum oven and coated with gold sputter before SEM analyses.

Statistical Analysis

All data were reported as mean ± standard deviation. One-way analysis of variance (ANOVA) was performed to validate the significant differences among the groups. All statistical analyses were performed using SAS 9.4 (Richmond, USA) and differences were considered significant in $p < 0.05$ [4, 17, 18].

Results

Characterization of Nanofibrous Scaffolds

Figure 1a shows SEM images of the samples. The presence of elastin in compositions changed the morphology of cross-linked fibers from straight in the scaffold without elastin to ribbon-like for the scaffolds with 5 and 10% elastin, as also reported in the previous researches [19, 20]. The cross-linking process increased the fiber diameter and pore size of the scaffolds

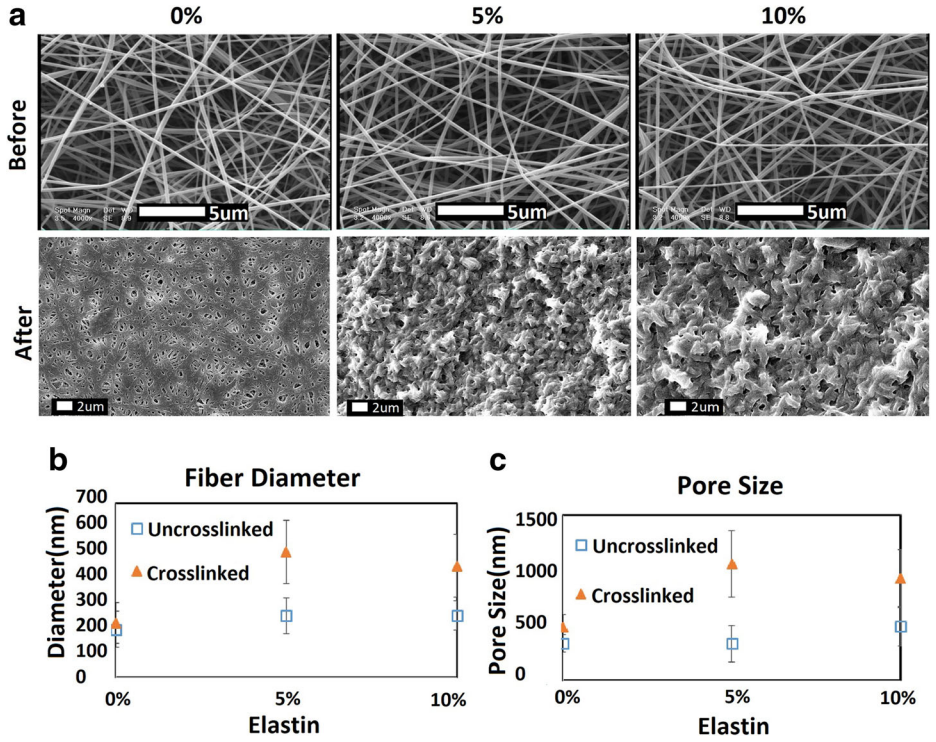

Fig. 1 **a** SEM micrographs of the gelatin/CA scaffolds with 0%, 5%, and 10% elastin. **b** Fiber diameter and **c** pore size of the scaffolds containing 0 to 10%wt elastin with and without cross-linking

in elastin-containing samples. Fusion of fibers together during the cross-linking and ribbon-like morphology of the elastin-based scaffolds caused these significant changes. Increasing the elastin content from 0 to 5% of gelatin enlarged the fiber diameter for the cross-linked scaffolds from 219 ± 80 nm to 505 ± 100 nm (Fig. 1b). Adding 10% elastin did not further enlarge the fiber diameter. The scaffold pore size was doubled in the scaffold with 5% elastin compared to gelatin/CA scaffold (Fig. 1c).

Chemical characterization of scaffolds was carried out using FTIR analysis to confirm the cross-linking of the fabricated nanofibers (Fig. 2a). The specific peaks of cellulose acetate including C-O-C (1240, 1160, and 1049 cm^{-1}), C=O (1745 cm^{-1}), and OH (broad peak between 3000 and 3700 cm^{-1}) were observed in all the samples, which confirms the presence of cellulose acetate in the scaffolds [4, 21]. According to functional group similarity of gelatin and elastin, it was expected to see some increase in amide I, II, III, and A peaks (1645, 1540, 1240, and 3300 cm^{-1}, respectively) with increasing elastin content in the composition, which is observable in Fig. 2a. The broad OH peak of all samples reveals the hydrogen bonding and miscibility of the components. Cross-linking reaction of gelatin and elastin within all the scaffolds was confirmed by the formation of the new CH=N bond at 1400 cm^{-1} due to aldimine absorption as previously reported elsewhere [22].

Swelling ratio of the cross-linked scaffolds was monitored during a period of 21 days in PBS. As shown in Fig. 2b, the swelling ratio of the scaffolds increased and then reached equilibrium during this period. This increase might be due to surface hydrogen bonding and the scaffold degradation. The swelling ratio of gelatin nanofibers was more than that of the

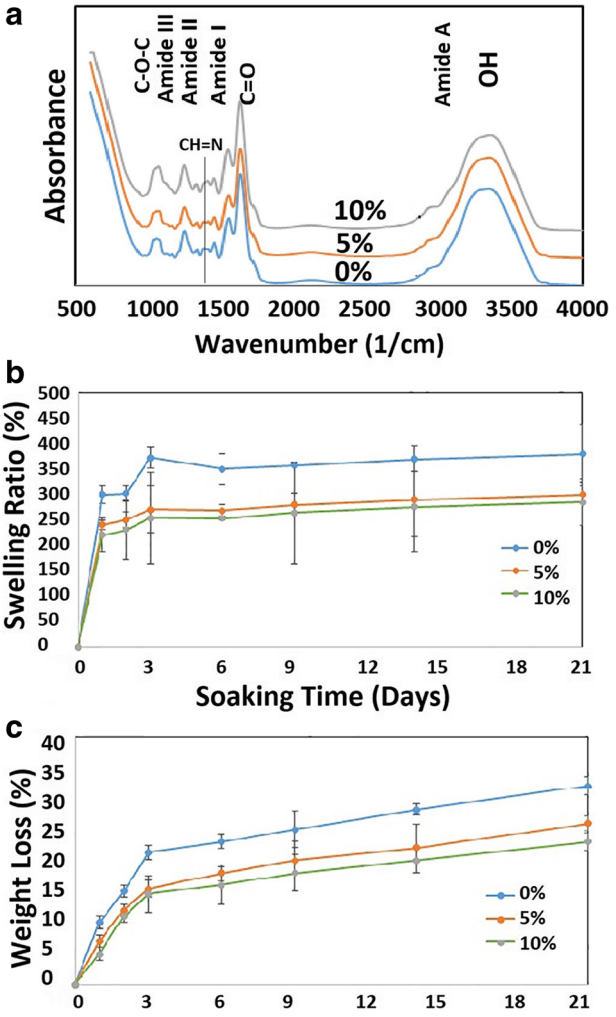

Fig. 2 **a** Chemical characterization of the scaffolds using FTIR analysis. **b** The swelling ratio of the scaffolds versus soaking time. **c** The weight loss of the scaffolds versus soaking time

scaffolds containing elastin. The percentage of swelling decreased from 380% in gelatin/CA scaffold to 285% in the scaffold containing 10% elastin. Increasing elastin from 5 to 10% had no significant effect on the swelling ratio. The presence of elastin in composition increased the fiber diameter. The diffusion of PBS into thicker fibers was slower due to the smaller surface-area-to-volume ratio. Vatankhah et al. reported the swelling ratio of about 400% for uncross-linked gelatin/CA scaffold [23]. It was expected to observe lower swelling ratio in cross-linked samples due to the consumption of hydrophilic amino groups during the cross-linking reaction as well as the higher stability of the polymeric network. It is worthy to note that the swelling ratio of a skin substitute is very important in wound exudation absorption [23]. Wang et al. measured the swelling ratio of four commercial skin substitutes including MEDPOR®, Hydro Coll®, DuoDERM®, and Tegaderm®. The values were reported in the range of 150 to 400%, respectively [24]. As shown in Fig. 2b, the swelling ratios of all the scaffolds were high enough to absorb the wound exudation as a skin substitute, which is possibly related to highly porous structure and hydrophilic composition of the scaffolds.

Both physical structure and chemical composition control the scaffold degradation rate. The elastin-containing scaffolds exhibited lower weight loss compared to elastin-free scaffold. The scaffold degradation occurred through the hydrolysis of amino acid groups in gelatin and elastin and the decomposition of the ester bond in cellulose acetate [15]. Figure 2c shows the weight loss of the cross-linked scaffolds during 21 days soaking in PBS. Increasing the amount of elastin from 0 to 10% increased the amino acid groups in the composition. Furthermore, physical structure of the scaffold including fiber diameter and pore size influenced the degradation rate of the scaffold, as also reported previously [15]. The increase in amino acid content and fiber diameter due to increasing the amount of elastin reduced the degradation rate.

Evaluation of mechanical properties of the prepared scaffolds at the wet condition better simulates the body condition. Therefore, the tensile modulus, ultimate tensile strength, and elongation at break of the samples were tested at the wet condition. Performing the test at wet condition simulates the body condition better. The tensile test was performed only on cross-linked samples, because of the high degradation rate of the uncross-linked samples in PBS. All samples showed a similar behavior; a linear trend followed by nonlinear one without any necking. Figure 3

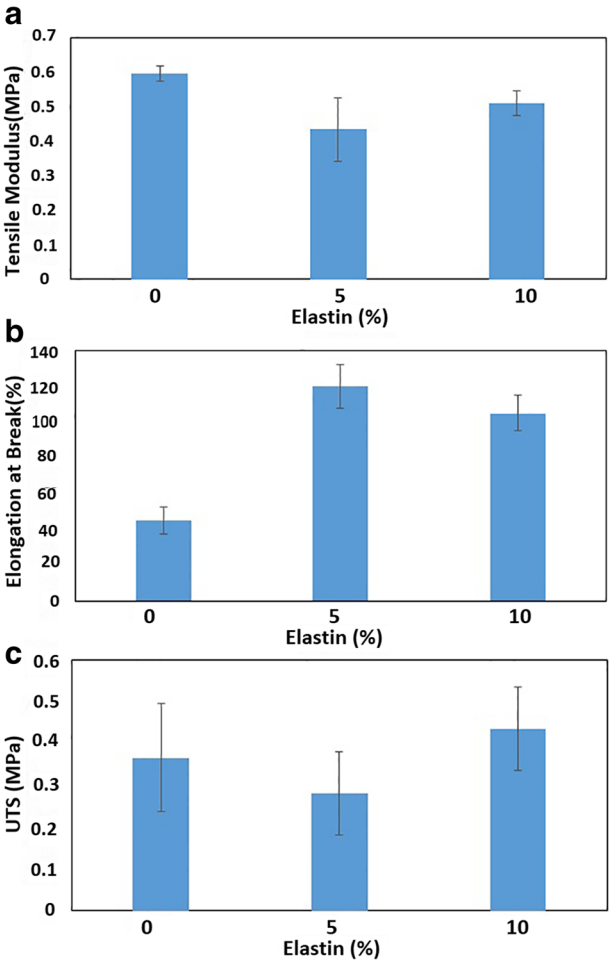

Fig. 3 **a** The tensile modulus, **b** elongation at break, and **c** ultimate tensile strength of the scaffolds in wet condition

shows the tensile properties of the scaffolds. Increasing the amount of elastin in composition from 0 to 5% decreased the tensile modulus whereas it increased the elongation at break of the scaffolds, significantly. But, further increasing from 5 to 10% had no significant effect on these tensile properties. The highest value of elongation was observed for the scaffold containing 5% elastin as much as 120%. A similar trend was observed in fiber diameter and scaffold pore size of the scaffolds. Increasing the elastin content from 0 to 5% of gelatin enlarged the fiber diameter and pore size of the scaffold, whereas further increasing elastin content to 10% had no significant effect on these physical properties. It has been reported that the tensile modulus of fibers with diameter lower than 500 nm decreased with increasing the fiber diameter [19, 25]. The amount of elastin had no significant effect on ultimate tensile strength (p value 0.58).

Cellular Viability, Attachment, and Proliferation

To assess the biological activity of the engineered scaffolds, dermal fibroblasts were cultured on the nanofibrous mats at 37 °C and 5% CO_2 for 7 days. Cellular metabolic activity was determined by the MTT assay as an indication of their viability. Live cells reduce the MTT compound to a colored formazan with absorbance at 570 nm. The absorbance quantity of formazan product is directly related to the number of viable cells on the sample. Figure 4a shows the absorbance percentage in the cells cultured on the fabricated scaffolds compared to the control (tissue culture plate). As shown in this figure, the absorbance percentage is higher in elastin-containing scaffolds during 7 days post seeding. The presence of elastin in the scaffolds did not induce toxicity and better supported fibroblast growth. Increasing elastin content from 5 to 10% had no significant effect on the amount of absorbance.

Cellular attachment and morphology on the scaffolds were also examined by SEM analysis (Fig. 4b). At day 1 after cell seeding, cells were attached and spread on the surface of scaffolds, and after 7 days, they proliferated on the surface and migrated through the scaffolds. As shown in Fig. 4b, fibroblast cells were better attached and grew in the elastin-containing scaffolds.

Discussion

Mimicking the chemical and mechanical properties of native ECM is critical for engineering scaffolds that support skin regeneration as more similar to native ECM is expected to increase cellular ingrowth. The skin ECM consists of collagen and elastin nanofibers in a polysaccharide matrix. Collagen and elastin make up 77% and 4% of the weight of the dried skin, respectively.

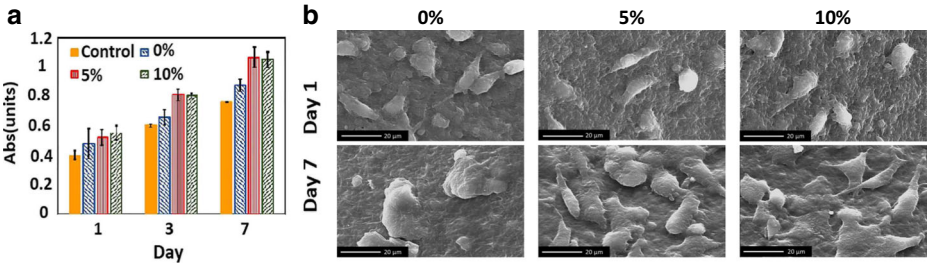

Fig. 4 **a** The absorbance percentage at 570 nm in the scaffolds in day 1, 3, and 7 after seeding. **b** The SEM micrographs of the scaffolds in days 1 and 7 after seeding fibroblast

Collagen fibers provide the stiffness of the ECM, and elastin renders it elastic [26]. Gelatin has been widely used as a substitute for collagen, because of their similarity and its availability [8–10]. Cellulose acetate is a polysaccharide with a long history in wound dressing applications [13, 14]. We optimized the composition and processing conditions for electrospinning of uniform gelatin/CA/elastin nanofibers. The main objective of this study was to study the effect of adding elastin to the composition on mechanical and biological properties of the fabricated scaffolds. Therefore, different amounts of elastin (0 to 10%wt) were loaded in gelatin/CA nanofibers to find the best composition for better ECM simulation. Nanofibrous webs with the diameter of 190 to 250 nm and pore size in the range of 330 to 500 nm were fabricated and were chemically cross-linked using glutaraldehyde vapor to increase their strength and degradation resistance. Glutaraldehyde has shown great success because of its availability and low cost in addition to its high reactivity with amine groups [27, 28]. The SEM micrographs and FTIR results confirm the cross-linking progress. The morphology of the scaffolds changed from separate fibers to the fused web. The fiber diameter and pore size of elastin-containing scaffolds increased due to cross-linking. Swelling of the fibers with glutaraldehyde vapor and fusion of the fibers together are the main reasons of the increases in diameter and pore size.

The largest fiber diameter and pore size were observed in the scaffold containing 5% elastin. The increasing pore size in electrospun scaffolds is an important feature which has gained attention in the last decade. Larger pores increase the possibility of cell infiltration into the scaffolds [19, 20, 29].

The swelling ratio is an important property in engineered scaffolds, which correlates to the bulk hydrophilicity of the scaffold. It influences transportation of nutrients and wound exudation. Over the limit swelling causes undesirable pressure to the near tissues and under the limit swelling ratio decreases the cell tendency to attach to the scaffold and cell nutrition. The incorporation of elastin in the composition slightly decreased the swelling ratio of the scaffolds. Overall, the swelling ratio of all the scaffolds was comparable to some commercial skin substitutes.

Mechanical properties of the engineered scaffolds are very important for better simulation of the ECM. The similarity of mechanical properties of the engineered scaffolds to the native tissue facilitates their integration and cellular ingrowth. In the literature, the range of skin Young's modulus has been reported to be between 0.2 and 1 MPa and skin can tolerate elongations more than 100% [26, 30]. Young's modulus of the scaffold containing 5%wt elastin was 0.43 ± 0.1 MPa, which was within this range. This scaffold also showed the highest value of elongation at break as much as 120%. Therefore, with adding 5%wt elastin to the blend of gelatin/CA, a ternary blend with similar composition and physicomechanical property to the native skin was reachable.

The presence of elastin also increased the cell interaction with the scaffolds. Great elasticity of these scaffolds or signaling events between proteins in scaffold composition and fibroblast cells increased the cell proliferation on these scaffolds. On the other hand, the larger pores in these scaffolds supported cellular to penetrate into the 3D structure of the scaffolds. Overall, results suggested that the gelatin/CA containing 5%wt elastin is a suitable candidate for skin tissue regeneration. The results should be later verified in animal studies.

Conclusion

The effect of elastin incorporation on physical, mechanical, and biological properties of gelatin/CA electrospun scaffolds was studied. The presence of elastin in the blend increased the fiber diameter and pore size of the scaffolds. The swelling ratio and degradation rate were decreased in elastin-containing scaffolds. The tensile modulus of the scaffolds was in the range of 0.4 to

0.6 MPa, which is appropriate for the skin regeneration. The highest value of elongation was observed for the scaffold containing 5% elastin as much as 120% strain. Further increasing elastin content to 10%wt had no significant effect on these properties. Therefore, the blend of gelatin with 30% CA and 5% elastin which had similar composition to the skin showed the best physicomechanical properties. MTT assay and SEM analysis also demonstrated the feasibility of using this composition for skin substitution and regeneration. Fibroblast cells interacted very well with this scaffold, so this scaffold can serve as a good candidate for skin tissue engineering.

Acknowledgments The authors would like to thank Research Institute in Biotechnology and Bioengineering at Isfahan University of Technology and Dental Sciences Research Center at Isfahan University of Medical Sciences.

Funding information This project received financial support from Bonyad Melli Nokhbegan (BMN).

Compliance with Ethical Standards

Conflict of Interest The authors declare that there is no conflict of interest.

References

1. Thomas, R., Soumya, K. R., Mathew, J., & Radhakrishnan, E. K. (2015). Electrospun polycaprolactone membrane incorporated with biosynthesized silver nanoparticles as effective wound dressing material. *Applied Biochemistry and Biotechnology, 176*(8), 2213–2224.
2. El-Aassar, M. R. E. f., El-Deeb, G. F., Shokry Hassan, N. M., & Mo, H. (2016). X. *Applied Biochemistry and Biotechnology, 178*(8), 1488–1502.
3. Groeber, F., Holeiter, M., Hampel, M., Hinderer, S., & Schenke-Layland, K. (2011). *Advanced Drug Delivery Reviews, 128*, 352–366.
4. Khalili, S. N. K., Razavi, S., Hashemi Beni, M., Heydari, B., & Tamayol, F. A. (2018). *Journal of Biomedical Materials Research. Part A, 106*(2), 370–376.
5. Khalili, S., Nouri Khorasani, S., Saadatkish, N., & Khoshakhlagh, K. (2016). *Polymer Science Series A, 58*(3), 399–408.
6. Annabi, N., Mithieux, S. M., Camci-Unal, G., Dokmeci, M. R., Weiss, A. S., & Khademhosseini, A. (2013). Elastomeric recombinant protein-based biomaterials. *Biochemical Engineering Journal, 77*, 110–118.
7. Hong, Y., Zhu, X., Wang, P., Fu, H., Deng, C., Cui, L., Wang, Q., & Fan, X. (2016). Tyrosinase-mediated construction of a silk fibroin/elastin nanofiber bioscaffold. *Applied Biochemistry and Biotechnology, 178*(7), 1363–1376.
8. Malafaya, P. B., Silva, G. A., & Reis, R. L. (2007). Natural–origin polymers as carriers and scaffolds for biomolecules and cell delivery in tissue engineering applications. *Advanced Drug Delivery Reviews, 59*(4-5), 207–233.
9. Bagherifard, S., Tamayol, A., Mostafalu, P., Akbari, M., Comotto, M., Annabi, N., Ghaderi, M., Sonkusale, S., Dokmeci, M. R., & Khademhosseini, A. (2016). Dermal patch with integrated flexible heater for on demand drug delivery. *Advanced Healthcare Materials, 5*(1), 175–184.
10. Najafabadi, A. H., Abdouss, M., & Faghihi, S. (2014). *Journal of Nanoparticle Research, 16*, 1–14.
11. Balakrishnan, B., Mohanty, M., Fernandez, A. C., Mohanan, P. V., & Jayakrishnan, A. (2006). Evaluation of the effect of incorporation of dibutyryl cyclic adenosine monophosphate in an in situ-forming hydrogel wound dressing based on oxidized alginate and gelatin. *Biomaterials, 27*(8), 1355–1361.
12. Cahú, T. B., Silva, R. A., Silva, R. P. F., Silva, M. M., Arruda, I. R. S., & Silva, J. F. (2017). Evaluation of chitosan-based films containing gelatin, chondroitin 4-sulfate and ZnO for wound healing. *Applied Biochemistry and Biotechnology, 183*(3), 765–777.
13. Khan, F., & Ahmad, S. R. (2013). Polysaccharides and their derivatives for versatile tissue engineering application. *Macromolecular Bioscience, 13*(4), 395–421.
14. Bačáková, L., Novotná, K., & Pařízek, M. (2014). *Physiological Research, 63*, S29–S47.

15. Kharaziha, M., Nikkhah, M., Shin, S. R., Annabi, N., Masoumi, N., Gaharwar, A. K., Camci-Unal, G., & Khademhosseini, A. (2013). PGS:Gelatin nanofibrous scaffolds with tunable mechanical and structural properties for engineering cardiac tissues. *Biomaterials, 34*(27), 6355–6366.
16. Venugopal, J., & Ramakrishna, S. (2005). Applications of polymer nanofibers in biomedicine and biotechnology. *Applied Biochemistry and Biotechnology, 125*(3), 147–158.
17. Neisiany, R. E., Khorasani, S. N., Naeimirad, M., Lee, J. K. Y., & Ramakrishna, S. (2017). Improving mechanical properties of carbon/epoxy composite by incorporating functionalized electrospun polyacrylonitrile nanofibers. *Macromol. Materials Engineering, 302*, 551.
18. Neisiany, R. E., Khorasani, S. N., Lee, J. K. Y., Naeimirad, M., & Ramakrishna, S. (2018). Interfacial toughening of carbon/epoxy composite by incorporating styrene acrylonitrile nanofibers. *Theoretical and Applied Fracture Mechanics, 95*, 242–247.
19. Rnjak-Kovacina, J., Li, S. W. Z., Maitz, P. K. M., Young, C. J., Wang, Y., & Weiss, A. S. (2011). Tailoring the porosity and pore size of electrospun synthetic human elastin scaffolds for dermal tissue engineering. *Biomaterials, 32*(28), 6729–6736.
20. Rnjak-Kovacina, J., & Weiss, A. S. (2011). Increasing the pore size of electrospun scaffolds. *Tissue Engineering. Part B, Reviews, 17*(5), 365–372.
21. Vallejos, M. E., Peresin, M. S., & Rojas, O. J. (2012). All-cellulose composite fibers obtained by electrospinning dispersions of cellulose acetate and cellulose nanocrystals. *Journal of Polymers and the Environment, 20*(4), 1075–1083.
22. Nguyen, T. H., & Lee, B. T. (2010). Fabrication and characterization of cross-linked gelatin electro-spun nano-fibers. *Journal of Biomedical Science and Engineering, 3*(12), 1117–1124.
23. Vatankhah, E., Prabhakaran, M. P., Jin, G., Ghasemi Mobarakeh, L., & Ramakrishna, S. (2013). *Journal of Biomaterials Applications, 28*, 909–921.
24. Wang, H. M., Chou, Y. T., Wen, Z. H., Wang, Z. R., Chen, C. H., & Ho, M. L. (2013). *PLoS One, 8*, 56330.
25. Mohammadzadehmoghadam, S., Dong, Y., & Davies, I. J. (2016). Modeling electrospun nanofibers: an overview from theoretical, empirical, and numerical approaches. *International Journal of Polymeric Materials and Polymeric Biomaterials, 65*(17), 901–915.
26. Wilkes, G. L., Brown, I. A., & Wildnauer, R. H. (1973). The biomechanical properties of skin. *Critical Reviews in Bioengineering, 4*, 453–495.
27. Nivison-Smith, L., Rnjak, J., & Weiss, A. S. (2010). Synthetic human elastin microfibers: stable cross-linked tropoelastin and cell interactive constructs for tissue engineering applications. *Acta Biomaterialia, 6*(2), 354–359.
28. Grover, C. N., Cameron, R. E., & Best, S. M. (2012). Investigating the morphological, mechanical and degradation properties of scaffolds comprising collagen, gelatin and elastin for use in soft tissue engineering. *Journal of the Mechanical Behavior of Biomedical Materials, 10*, 62–74.
29. Vaquette, C., & Cooper-White, J. J. (2011). Increasing electrospun scaffold pore size with tailored collectors for improved cell penetration. *Acta Biomaterialia, 7*(6), 2544–2557.
30. Pawlaczyk, M., Lelonkiewicz, M., & Wieczorowski, M. (2013). Age-dependent biomechanical properties of the skin. *Postepy Dermatologii Alergologii, 30*(5), 302–306.

Affiliations

Shahla Khalili[1,2] · Saied Nouri Khorasani[1] · Seyed Mohammad Razavi[3] · Batool Hashemibeni[4] · Ali Tamayol[2]

[1] Department of Chemical Engineering, Isfahan University of Technology, Isfahan 84156-83111, Iran

[2] Center for Biomedical Engineering, Department of Medicine, Brigham and Women's Hospital, Harvard Medical School, Boston, MA 02139, USA

[3] Department of Oral and Maxillofacial Pathology, School of Dentistry and Torabinejad Dental Research Center, Isfahan University of Medical Sciences, Isfahan, Iran

[4] Department of Anatomical Sciences, Medical School, Isfahan University of Medical Sciences, Isfahan 81746-73461, Iran